# Damping of spinful excitons in LaCoO₃ by thermal fluctuations: Theory and experiment

Atsushi Hariki [●],[1,2] Ru-Pan Wang,[3] Andrii Sotnikov [●],[1,4] Keisuke Tomiyasu [●],[5,6] Davide Betto,[7] Nicholas B. Brookes,[7]
Yohei Uemura [●],[3] Mahnaz Ghiasi,[3] Frank M. F. de Groot,[3] and Jan Kuneš [●][1,8]

[1]*Institute of Solid State Physics, TU Wien, 1040 Vienna, Austria*
[2]*Department of Physics and Electronics, Graduate School of Engineering, Osaka Prefecture University 1-1 Gakuen-cho,*
*Nakaku, Sakai, Osaka 599-8531, Japan*
[3]*Debye Institute for Nanomaterials Science, Utrecht University, Universiteitsweg 99, 3584 CG Utrecht, Netherlands*
[4]*Akhiezer Institute for Theoretical Physics, NSC KIPT, Akademichna 1, 61108 Kharkiv, Ukraine*
[5]*Department of Physics, Tohoku University, Aoba, Sendai 980-8578, Japan*
[6]*NISSAN ARC, LTD., 1, Natsushima-cho, Yokosuka, Kanagawa 237-0061, Japan*
[7]*European Synchrotron Radiation Facility, 71 Avenue des Martyrs, CS40220, F-38043 Grenoble Cedex 9, France*
[8]*Institute of Physics, Czech Academy of Sciences, Na Slovance 2, 182 21 Praha 8, Czech Republic*

We present Co $L_3$-edge resonant inelastic x-ray scattering (RIXS) of bulk LaCoO₃ across the thermally induced spin-state crossover around 100 K. Owing to a high energy resolution of 25 meV, we observe unambiguously the dispersion of the intermediate-spin (IS) excitations in the low-temperature regime. Approaching the intermediate temperature regime, the IS excitations are damped and the bandwidth is reduced. The observed behavior can be well described by a model of mobile IS excitons with strong attractive interaction, which we solve by using dynamical mean-field theory for hard-core bosons. Our results provide a detailed mechanism of how high-spin and IS excitations interact to establish the physical properties of cobaltite perovskites.

## I. INTRODUCTION

The physics of ionic insulators at energies below the band gap opened between fully occupied and empty atomic states is often trivial. Under certain conditions, electron-electron interactions may alter this picture by giving rise to low-energy bosonic excitations. This is the case of LaCoO₃, a structurally simple quasicubic material with complex magnetic and transport properties studied since the 1950s [1–7].

LaCoO₃, a diamagnetic insulator with a low-spin (LS, $S = 0$, $^1A_{1g}$) ground state and a band gap between filled $t_{2g}^6$ and empty $e_g^0$ subshells, becomes a paramagnetic insulator around 100 K. This behavior is traditionally attributed to thermal population of excited atomic multiplets. The high-spin (HS, $S = 2$, $t_{2g}^4 e_g^2$, $^5T_{2g}$) or intermediate-spin (IS, $S = 1$, $t_{2g}^5 e_g^1$, $^3T_{1g}$) nature of the lowest excited state has been the subject of an ongoing debate [7–19]. Both HS and IS scenarios evoke an important question. Decorating the lattice with excited atoms leads to sizable distribution Co–O bond lengths due to breathing distortion around HS atoms or Jahn-Teller distortion around IS atoms. At experimentally reported concentrations, the excited atoms are expected to form a regular lattice, an effect favored by electron-lattice coupling [20,21], as well as electronic correlations [22–24]. Nevertheless, no spin-state order nor Co-O bond-length disproportionation was observed in LaCoO₃ [25]. This leaves the possibility of dynamically fluctuating spin-state order [26], for which, however, the picture of thermal atom-bound excitations provides no mechanism.

Recently, a model of LaCoO₃ was proposed [27], in which the IS excitations are viewed as mobile bosons (excitons) carrying spin $S = 1$; see Fig. 1(g). Band-structure calculations and experimental evidence lead to an estimated excitonic half bandwidth of 250 meV, comparable to the IS on-site energy of about $\epsilon_{IS} = 340$ meV. The HS excitations are viewed as immobile $S = 2$ biexcitons with an energy of about $\epsilon_{HS} = 20$ meV [15,28]; see Fig. 2. This implies a strong attraction $V$ between IS excitons, $\epsilon_{HS} \approx 2\epsilon_{IS} - V$.

RIXS experiments performed at low temperature matched nicely the generalized spin-wave theory based on first-principle parameters [29] and confirmed the estimate of Ref. [27]. The low-temperature RIXS measurements map out the dynamics of a single IS or HS excitation on the LS lattice (ground state), i.e., a single-boson problem. The strong-coupling nature of the model [27] suggests a sizable temperature dependence of the excitation spectrum when excited states start being populated.

In this paper, we report the thermal evolution of the IS dispersion in LaCoO₃ obtained with Co $L_3$-RIXS and its theoretical modeling using dynamical mean-field theory for hard-core bosons (HB-DMFT). Our main results are (i) the observation of the low-temperature IS dispersion in the 0.2–0.5 eV range in the accessible part of the Brillouin zone with a high energy resolution, (ii) observation of "melting" of the sharp IS dispersion into a narrow band of damped excitations at elevated temperatures, and (iii) theoretical modeling of the observed behavior by a multiflavor attractive Hubbard model for hard-core bosons.
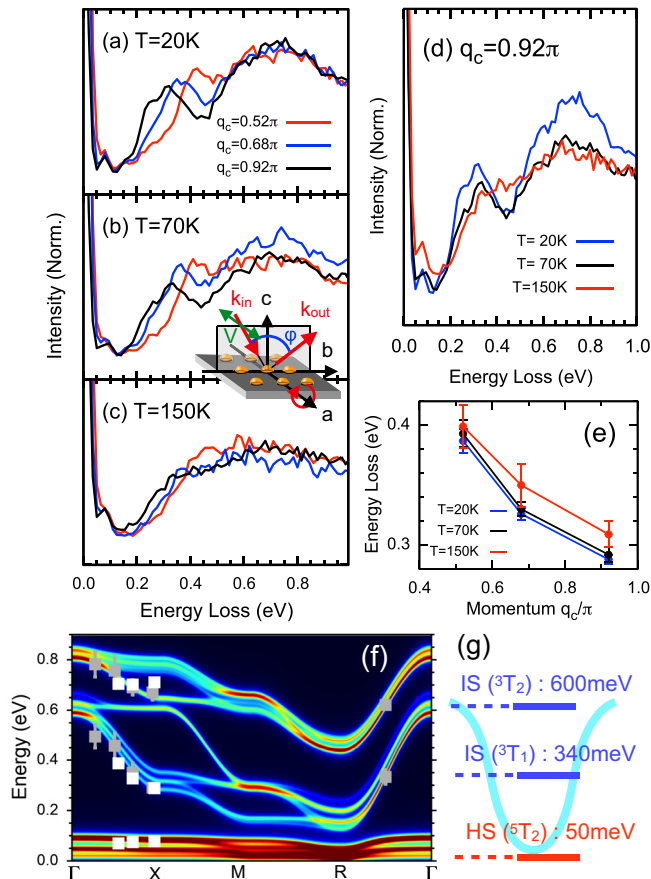
FIG. 1. The experimental RIXS intensities for selected $q = (0, 0, q_c)$ measured at (a) 20 K, (b) 70 K, and (c) 150 K. (d) Temperature dependence at $q_c = 0.92\pi$. Two distinct features located at 200–500 and 800 meV correspond to the $^3T_{1g}$ and $^3T_{2g}$ IS excitations [29], respectively. The experimental geometry and the definition of angle $\varphi$ are illustrated in the inset. (e) The peak position of the $^3T_{1g}$ IS excitation obtained by the fitting analysis, see SM [30]. (f) Comparison at 20 K between theory (color map), present RIXS data with $\Delta E = 25$ meV (white), and previous RIXS data with $\Delta E = 90$ meV (gray) [29]. (g) Sketch of the excitonic scenario: the atomic-level energies and the IS dispersion on the LS background.
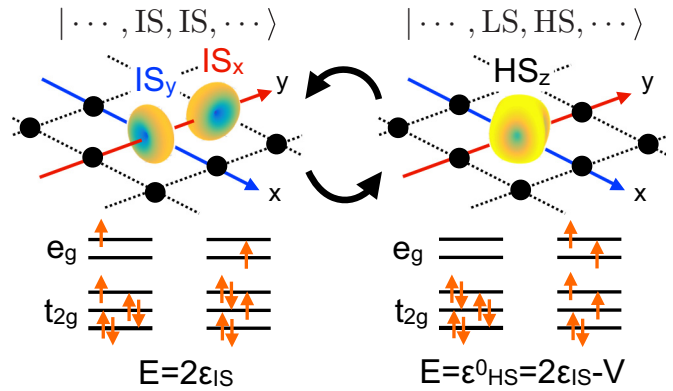


FIG. 2. Sketch of the IS exciton ($IS_{x,y}$, ellipses correspond to the charge distribution) propagation on the LS (black circles) and the formation of the immobile HS biexciton ($HS_z$). $IS_x$ ($IS_y$) excitons with the $d_{yz} \otimes d_{y^2-z^2}$ ($d_{zx} \otimes d_{z^2-x^2}$) character in the IS ($^3T_{1g}$) manifolds propagate in the $yz$ ($xz$) plane [27,29,32]. $IS_z$ exciton (not shown) with the $d_{xy} \otimes d_{x^2-y^2}$ character propagates in the $xy$ plane. The HS biexciton can be formed (melted) by (into) two IS excitons via the local attractive interaction between IS excitons.

$(0, 0, 0.68\pi)$, and $(0, 0, 0.92\pi)$, respectively. Details of the sample preparation and the data analysis including fitting can be found in the Supplemental Material (SM) [30].

Our main observations are summarized in Fig. 1. The RIXS spectra exhibit low-energy features observed in previous studies [28,29]. At 20 K, we observe a clear dispersion of the peak in 0.2–0.5 eV range that was assigned to the IS ($^3T_{1g}$) excitation [28,29]. The HS ($^5T_{2g}$) excitation observed below 0.1 eV shows no dispersion. The IS dispersion is consistent with the theory and experiment of Ref. [29], see Fig. 1(f), with substantially reduced error bars, provided by the present high energy resolution. Increasing the temperature above 100 K leads to a distinct narrowing and smearing of the dispersive feature, see Figs. 1(b)–1(e). Other spectroscopic studies [7,28] indicated growing concentration of HS excitations with temperature, while the system remains a spatially uniform insulator. Thus theoretical modeling of the heating effect on the dispersive IS excitations is a challenge that we address next.

## III. THEORY

An efficient description of the insulating LaCoO₃ is provided by a low-energy effective model of the LS ground state and its bosonic IS and HS excitations. Such a model was constructed in Ref. [29] starting from density-functional theory. Despite substantial simplification, the bosonic model poses a strongly interacting problem, except for the lowest temperatures $T \approx 0$, where thermal excitations vanish and the interactions between them does not matter. The RIXS final state at $T \approx 0$ is a single IS (or HS) state excited on the LS lattice, a state that can be described with a generalized linear spin-wave theory [29]; see Fig. 1(f).

At elevated temperatures, the strongly interacting excitations must be taken into account. A direct treatment of the model of Ref. [29] with 24 states per each Co atom is technically hopeless and obscuring the key physics. Therefore

## II. EXPERIMENT

Co $L_3$-edge RIXS was measured on the beamline ID32 at the European Synchrotron Radiation Facility (ESRF) [31]. The energy resolution $\Delta E$ was 25 meV. We recorded RIXS spectra at 20, 70, and 150 K. Note that 20 K (150 K) is well below (above) the spin-state crossover temperature of 80–100 K. The experimental geometry is illustrated in Fig. 1. The RIXS measurements were carried out in the $bc$ scattering plane by rotating the sample around the $a$ axis, with linearly polarized x-rays (vertical to the $bc$ scattering plane). The sample normal is aligned to the $c$ axis of the (pseudo) cubic crystal with the lattice constant $a_{cub} \approx 3.83$ Å. In this setup, we can measure a momentum transfer of $\mathbf{q} = (0, 0, q_c)/a_{cub}$. Hereafter, $a_{cub}$ is omitted for simplicity. The x-ray wavelength at the Co $L_3$ edge in LaCoO₃ ($\approx 15.9$ Å) determines the accessible $|\mathbf{q}|$ values. The spectra were taken at $\varphi = 115°$, 90°, and 35°, corresponding to $\mathbf{q} = (0, 0, 0.52\pi)$,

we simplify the model to the essential minimum: (i) we neglect the spin structure of the problem, (ii) we neglect the spin-orbit coupling, (iii) we approximate the HS excitation as two IS excitations on the same site, (iv) we use the DMFT approximation [33,34]. Our model has the form of three-flavor bosonic Hubbard Hamiltonian on a cubic lattice

$$\hat{H} = \epsilon_{IS} \sum_{\mathbf{i}} \sum_{\alpha} \hat{n}_{\mathbf{i},\alpha} - V \sum_{\mathbf{i}} \sum_{\alpha > \beta} \hat{n}_{\mathbf{i},\alpha} \hat{n}_{\mathbf{i},\beta}$$

$$+ t \sum_{\mathbf{i}} \sum_{\alpha,\beta} (1 - \delta_{\alpha\beta}) \hat{b}^{\dagger}_{\mathbf{i}\pm\mathbf{e}_{\beta},\alpha} \hat{b}_{\mathbf{i},\alpha}. \tag{1}$$

The vacuum of the model represents the global LS state $|\emptyset\rangle = \prod_{\mathbf{i}} |LS_{\mathbf{i}}\rangle$. Bosonic $\hat{b}^{\dagger}_{\mathbf{i},\gamma}$ operators create the IS excitations $|IS_{\mathbf{i},\gamma}\rangle \equiv \hat{b}^{\dagger}_{\mathbf{i},\gamma}|\emptyset\rangle$ with the orbital symmetry $\varepsilon_{\alpha\beta\gamma} d_{\alpha\beta} \otimes d_{\alpha^2-\beta^2}$, with $\alpha$, $\beta$, $\gamma$ from $\{x, y, z\}$ and $\varepsilon_{\alpha\beta\gamma}$ being the fully antisymmetric tensor. HS excitations are represented by a doubly occupied sites $|HS_{\mathbf{i},\gamma}\rangle \equiv \|\varepsilon_{\alpha\beta\gamma}\| \hat{b}^{\dagger}_{\mathbf{i},\alpha} \hat{b}^{\dagger}_{\mathbf{i},\beta}|\emptyset\rangle$. The Pauli principle of the underlying fermionic problems leads to kinematic hardcore constraints of maximum one boson of a given flavor and a maximum total of two bosons per site. The constraints can be enforced explicitly or dynamically by introducing an additional on-site interaction $U \sum_{\mathbf{i}} [\sum_{\alpha}(1 - \hat{n}_{\mathbf{i}\alpha})\hat{n}_{\mathbf{i}\alpha} + \hat{n}_{\mathbf{i}x}\hat{n}_{\mathbf{i}y}\hat{n}_{\mathbf{i}z}]$ with $U \to \infty$. The $b$ excitations can propagate by hopping to nearest-neighbor sites in direction $\mathbf{e}_{\alpha}$. Due to the shape of the $T_{1g}$ excitations, the hopping of $IS_{\gamma}$ along the $\gamma$ axis is negligible compared with the two perpendicular directions.

To summarize, the model describes a gas of mobile bosons of three flavors ($T_{1g}$ IS) that interact via local attractive (interflavor) interaction. The LS → IS transition at a x-ray excited Co atom in RIXS corresponds to creating a boson in (1). The $T_{1g}$ IS part of the RIXS spectra therefore corresponds to the positive frequency part of the single-particle spectral function of the $b$ bosons in the model.

We use the following model parameters $t = 58$ meV, $\epsilon_{IS} = 340$ meV, $V = 620$ meV. The values of $\epsilon_{IS}$ and $t$ were obtained in Ref. [29] by a combination of first-principles calculation and RIXS analysis. Nevertheless, their magnitudes can be estimated by using the established values of crystal-field splitting, Hund's exchange, and $e_g$ ($t_{2g}$) bandwidths in LaCoO₃ together with the experimental fact of stability of the LS ground state and activation energies of low-lying excited states. The present $\epsilon_{IS}$ compares well to the estimate provided by ligand-field analysis [7]. The value of $t$ reflects the hopping amplitudes (bandwidths) of the $t_{2g}$ and $e_g$ electrons in LaCoO₃ [27], while it depends to some extent on the effective Hubbard repulsion within the Co $3d$ shell (determined by matching to the RIXS experiment [29]). The value of $V$ is strongly constrained by the basic fact of stability of the LS ground state and existence of HS excitations at 15–20 meV [7,15]. This implies $0 \lesssim \epsilon^0_{HS} = 2\epsilon_{IS} - V$. It is the interaction $V$ that appears in our theory, whereas the more natural parameter $\epsilon^0_{HS}$ is used in the following discussion, although it is not directly experimentally observable, as will be become clear later.

We treat model (1) by using the bosonic DMFT [34–37] with strong-coupling continuous-time quantum Monte Carlo (CT-QMC) impurity solver [36,38]. The hard-core constraint can be implemented dynamically by introducing a large in-
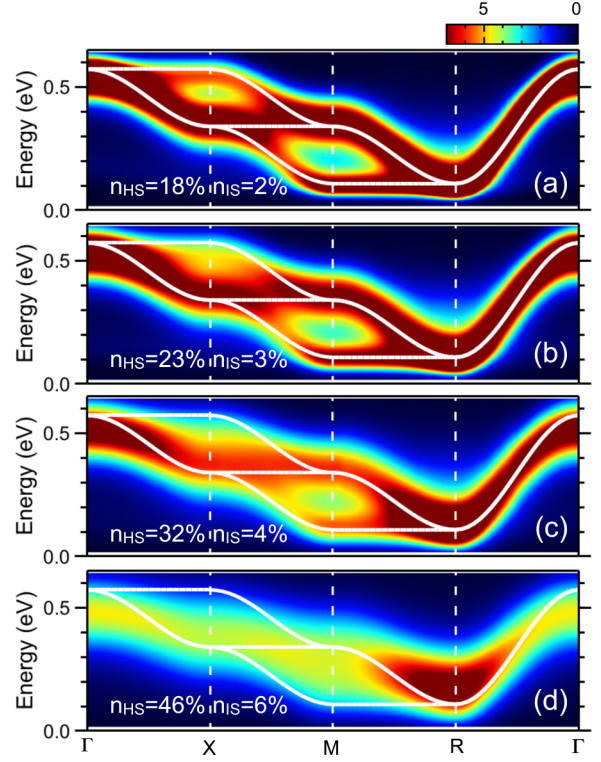


FIG. 3. The $k$-resolved excitation spectra of the attractive Hubbard model obtained by HB-DMFT for various HS and IS populations at $V = 620$ meV and (a) $\beta = 80$, (b) $\beta = 60$, (c) $\beta = 40$, and (d) $\beta = 20$. Here $\beta$ is the inverse temperature, $\beta = 1/k_B T$. The white line indicates the noninteracting dispersion at 0 K.

traflavor interaction or explicitly.[1] Nevertheless, the explicit constraint has numerical advantages and is more elegant. While enforcing the constraint in the CT-QMC calculation is straightforward, care must be taken with the definition of self-energy, because the Green's function does not have the canonical $\frac{1}{i\omega_n}$ high-frequency limit due to the constraint. An analogous problem arising in the $t - J$ model for fermions was discussed by Shastry [39] and Perepelitsky and Shastry [40], who introduced the concept of extremely correlated Fermi liquid and a modified Dyson equation, which for bosons takes the form

$$G_{\mathbf{k},\gamma}(i\omega_n) = \frac{1 - \eta}{i\omega_n - (1 - \eta)\epsilon_{\mathbf{k},\gamma} - \Sigma(i\omega_n)}, \tag{2}$$

where $\eta$ measures the spectral weights missing due to the hard-core constraint and is given as $\eta = 2\langle\hat{n}_{\alpha}\rangle + 2\langle\hat{n}_{\alpha}\hat{n}_{\beta}\rangle_{\alpha\neq\beta}$, where the occupations are equal for all flavors. We refer the reader interested in technical details to the SM [30] and focus herein on discussing the results.

---

[1]We have checked on several cases that both approaches lead to the same low-energy spectral functions and excitation concentrations; see SM [30].

## IV. DISCUSSION

Figures 3(a)–3(d) show the evolution of the positive-frequency part of $k$-resolved spectral function $A_{\mathbf{k},\gamma}(\omega) = -\frac{1}{\pi} \operatorname{Im} G_{\mathbf{k},\gamma}(\omega^+)$ with temperature $T$. Despite its simplicity, the model (1) captures the essential features of the experimental data [Figs. 1(a)–1(d)]. At $T = 0$ the system is in its vacuum ground state (all atoms in the LS state) and the spectrum consists of three bands with $\epsilon_{\mathbf{k},\gamma} = \epsilon_{IS} + 2t \sum_\alpha (1 - \delta_{\alpha\gamma}) \cos k_\alpha$ dispersion indicated by white lines. This dispersion, by construction, reproduces the $T_{1g}$ part of the spectrum in Fig. 1(f) except for the effect of the spin-orbit coupling neglected in model (1). The HB-DMFT spectrum in Fig. 3(a) taken at slightly elevated temperature closely resembles the $T = 0$ spectrum. Heating the system further, the equilibrium state changes due thermal population of the excited states. These are dominantly HS excitations, the doubly occupied sites $n_{HS} = \langle \hat{n}_x \hat{n}_y \rangle + \langle \hat{n}_y \hat{n}_z \rangle + \langle \hat{n}_z \hat{n}_x \rangle$. The IS population, i.e., the concentration of singly occupied sites $n_{IS} = \langle \hat{n}_x \rangle + \langle \hat{n}_y \rangle + \langle \hat{n}_z \rangle - 2n_{HS}$, is nine to seven times smaller. Increasing concentration of the excitations results in band narrowing, broadening of the spectral lines, and spectral weight redistribution; see Figs. 3(c) and 3(d).

When accessing the role of the attractive interaction $V$, one has to consider that even a model with $V = 0$ exhibits some $T$ dependence of the spectrum due to the kinematic hard-core constrains. However, the thermal population of the excited states for $V = 0$ remains small in the studied temperature range and the $T$ dependence of the spectra is negligible. Formation of HS excitations, represented by strong attractive $V$, is thus crucial for the observed behavior of the RIXS spectra.

As discussed in Refs. [27,29], the HS excitation is expected to be almost immobile and thus well described with a $k$-independent excitation energy, $\epsilon_{HS}^0$ in case of an isolated Co atom. This changes on the lattice. To quantify this effect, we define a $T$-dependent effective activation energy $\epsilon_{HS}(T)$. It is the excitation energy in a hypothetical isolated atom with the LS ground state and three excited HS states (HS$_x$, HS$_y$, HS$_z$), which leads to the same HS population $n_{HS}(T)$ as the lattice model at a given temperature $T$,

$$\epsilon_{HS}(T) = T \ln \frac{3 - 3n_{HS}(T)}{n_{HS}(T)}. \tag{3}$$

In Fig. 4 we show $\epsilon_{HS}(T)$ as well as $\epsilon_{HS}(n_{HS})$ dependencies for interaction strength $V$ and compare them with available experimental data [7,28]. We find that the low-$T$ value of $\epsilon_{HS}$ (an isolated HS excitation on a lattice) is substantially smaller than $\epsilon_{HS}^0$ (HS excitation in an isolated atom). The explanation of this observation is straightforward. While the HS excitation is a stable bound state, it is not localized on a single atom. Quantum fluctuations on the adjacent nearest-neighboring bonds of the type $|HS, LS\rangle \rightleftarrows |IS, IS\rangle$, see Fig. 2, lower its energy. A simple perturbation theory gives an estimate $\epsilon_{HS}^0 - \epsilon_{HS} \approx 8t^2/V \approx 40$ meV, which describes the calculated data quite well. It should be pointed out that the on-site energies $\epsilon_{IS}$ and $\epsilon_{HS}^0$ entering Eq. (1) are not purely atomic energies, but contain renormalization due to virtual electron hopping [29,41].
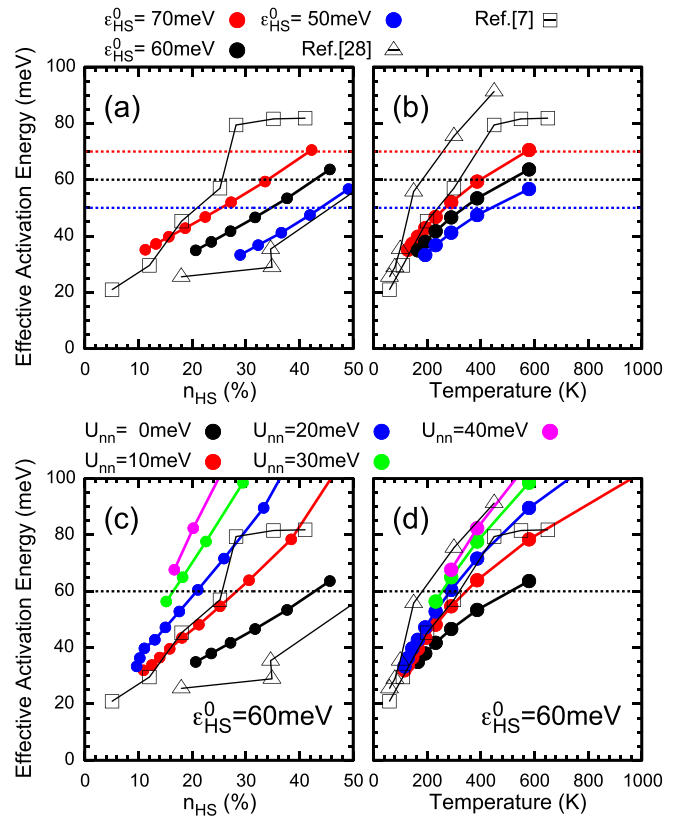


FIG. 4. The calculated effective activation energies for (a) $n_{HS}$ and (b) temperatures. The different colors correspond to different bare HS energies $\epsilon_{HS}^0 = 70$ meV ($V = 610$ meV), 60 meV ($V = 620$ meV), and 50 meV ($V = 630$ meV), additionally indicated by horizontal dashed lines. The experimental estimates [7,28] are provided. (c), (d) $\epsilon_{HS}(T)$ at different intersite interactions $U_{nn}$ for $\epsilon_{HS}^0 = 60$ meV.

Similar to the experimental observations, we find that $\epsilon_{HS}$ increases with temperature. The calculated $d\epsilon_{HS}/dT$ has a realistic order of magnitude, but is smaller than the experimental observations [7,28]. This is not unexpected. The increase of $\epsilon_{HS}$ with $n_{HS}$ is generally accepted to be caused by nearest-neighbor HS-HS repulsion, which originates from blocking of virtual electron hopping [22–24,42] and possibly electron-lattice coupling [20]. The strong-coupling model of Ref. [29] captures the former effect. Within the biexciton picture of the HS state, the HS-HS repulsion is inherited from the nearest-neighbor repulsion of the underlying IS excitons. Similar to their hopping amplitudes (1), the IS nearest-neighbor repulsion is strongly anisotropic, inheriting the anisotropy of the constituting electronic orbitals.

A simple, although approximate, way to include the intersite repulsion in our model is a static mean-field treatment. Following this approach, we consider only the dominant nearest-neighbor repulsion between the excitons of the same flavor within the their hopping plane $H_{nn} = U_{nn} \sum_{\mathbf{i}} \sum_{\alpha,\beta} (1 - \delta_{\alpha\beta}) \hat{n}_{\mathbf{i}+\mathbf{e}_\beta, \alpha} \hat{n}_{\mathbf{i},\alpha}$. The results in Figs. 4(c) and 4(d) demonstrate that inclusion of the intersite repulsion indeed improves the agreement with experimental estimates. The additional term does not change the character of the spectra in Fig. 3, as it

simply introduces a $T$ dependent and self-consistently determined $\epsilon_{IS}$ in Eq. (1). We point out that the static mean-field approximation is rather crude because it overestimates the effect of the repulsion, especially at low excitation densities, where it ignores the freedom of the excitons to efficiently avoid each other. This is reflected by the rather small value of $U_{nn}$ needed, while the strong-coupling estimates are in 100–200 meV range (depending on the spin configuration).

## V. CONCLUSIONS

In summary, by measuring Co $L_3$-RIXS of LaCoO₃ with state-of-the-art energy resolution, we have demonstrated a sizable mobility of $^3T_{1g}$ IS excitations. Melting of the corresponding dispersion into a narrow band of damped excitations, observed between 70 and 150 K, points to a strongly interacting nature of the IS excitations. The experimental data are well described by a gas of mobile IS excitons and immobile HS biexcitons, in contrast with the paradigm of atom-bound (immobile) IS or HS excitations. Our numerical results show that, even at low temperatures, where the IS concentration is negligible, virtual fluctuations $|HS, LS\rangle \rightleftarrows |IS, IS\rangle$ on the nearest-neighbor bonds play an important role. Dressing of HS excitations with a cloud of IS excitations on the neighboring atoms, Fig. 2, explains the recent inelastic neutron measurements [43], which reported delocalized magnetic form factors in LaCoO₃ and short-range ferromagnetic correlation at intermediate temperatures. Low theoretical

IS concentrations obtained at elevated temperatures suggest that the equilibrium state of LaCoO₃ can be described entirely in terms of dressed HS excitations. The IS excitations cannot be neglected as they mediate the intersite interactions between these HS excitations. This conclusion relies on the high mobility of IS excitations and is not sensitive to the exact value of IS excitation energy as long as the deviation from the present estimate is smaller than the difference $\epsilon_{IS} - \epsilon_{HS}$. The classic cobaltite question of whether the low-energy physics is determined by HS or IS excitations is therefore ill posed since both have to be taken into account.

[1] J. B. Goodenough, J. Phys. Chem. Solids **6**, 287 (1958).

[2] R. Heikes, R. Miller, and R. Mazelsky, Physica **30**, 1600 (1964).

[3] P. M. Raccah and J. B. Goodenough, Phys. Rev. **155**, 932 (1967).

[4] M. Abbate, J. C. Fuggle, A. Fujimori, L. H. Tjeng, C. T. Chen, R. Potze, G. A. Sawatzky, H. Eisaki, and S. Uchida, Phys. Rev. B **47**, 16124 (1993).

[5] K. Asai, A. Yoneda, O. Yokokura, J. M. Tranquada, G. Shirane, and K. Kohn, J. Phys. Soc. Jpn. **67**, 290 (1998).

[6] S. Stølen, F. Grønvold, H. Brinks, T. Atake, and H. Mori, Phys. Rev. B **55**, 14103 (1997).

[7] M. W. Haverkort, Z. Hu, J. C. Cezar, T. Burnus, H. Hartmann, M. Reuther, C. Zobel, T. Lorenz, A. Tanaka, N. B. Brookes, H. H. Hsieh, H.-J. Lin, C. T. Chen, and L. H. Tjeng, Phys. Rev. Lett. **97**, 176405 (2006).

[8] Y. Tanabe and S. Sugano, J. Phys. Soc. Jpn. **9**, 766 (1954).

[9] F. M. F. de Groot, J. C. Fuggle, B. T. Thole, and G. A. Sawatzky, Phys. Rev. B **42**, 5459 (1990).

[10] C. Zobel, M. Kriener, D. Bruns, J. Baier, M. Grüninger, T. Lorenz, P. Reutler, and A. Revcolevschi, Phys. Rev. B **66**, 020402(R) (2002).

[11] A. Ishikawa, J. Nohara, and S. Sugai, Phys. Rev. Lett. **93**, 136401 (2004).

[12] M. A. Korotin, S. Y. Ezhov, I. V. Solovyev, V. I. Anisimov, D. I. Khomskii, and G. A. Sawatzky, Phys. Rev. B **54**, 5309 (1996).

[13] J.-Q. Yan, J. S. Zhou, and J. B. Goodenough, Phys. Rev. B **69**, 134409 (2004).

[14] Z. Ropka and R. J. Radwanski, Phys. Rev. B **67**, 172401 (2003).

[15] A. Podlesnyak, S. Streule, J. Mesot, M. Medarde, E. Pomjakushina, K. Conder, A. Tanaka, M. W. Haverkort, and D. I. Khomskii, Phys. Rev. Lett. **97**, 247208 (2006).

[16] S. Noguchi, S. Kawamata, K. Okuda, H. Nojiri, and M. Motokawa, Phys. Rev. B **66**, 094404 (2002).

[17] G. Maris, Y. Ren, V. Volotchaev, C. Zobel, T. Lorenz, and T. T. M. Palstra, Phys. Rev. B **67**, 224423 (2003).

[18] T. Vogt, J. A. Hriljac, N. C. Hyatt, and P. Woodward, Phys. Rev. B **67**, 140401(R) (2003).

[19] T. Saitoh, T. Mizokawa, A. Fujimori, M. Abbate, Y. Takeda, and M. Takano, Phys. Rev. B **55**, 4257 (1997).

[20] R. A. Bari and J. Sivardière, Phys. Rev. B **5**, 4466 (1972).

[21] K. Knížek, Z. Jirák, J. Hejtmánek, P. Novák, and W. Ku, Phys. Rev. B **79**, 014430 (2009).

[22] J. Kuneš and V. Křápek, Phys. Rev. Lett. **106**, 256401 (2011).

[23] M. Karolak, M. Izquierdo, S. L. Molodtsov, and A. I. Lichtenstein, Phys. Rev. Lett. **115**, 046401 (2015).

[24] G. Zhang, E. Gorelov, E. Koch, and E. Pavarini, Phys. Rev. B **86**, 184413 (2012).

[25] P. G. Radaelli and S.-W. Cheong, Phys. Rev. B **66**, 094408 (2002).

[26] A. Doi, J. Fujioka, T. Fukuda, S. Tsutsui, D. Okuyama, Y. Taguchi, T. Arima, A. Q. R. Baron, and Y. Tokura, Phys. Rev. B **90**, 081109(R) (2014).

[27] A. Sotnikov and J. Kuneš, Sci. Rep. **6**, 30510 (2016).

[28] K. Tomiyasu, J. Okamoto, H. Y. Huang, Z. Y. Chen, E. P. Sinaga, W. B. Wu, Y. Y. Chu, A. Singh, R.-P. Wang, F. M. F. de

Groot, A. Chainani, S. Ishihara, C. T. Chen, and D. J. Huang, Phys. Rev. Lett. **119**, 196402 (2017).

[29] R. P. Wang, A. Hariki, A. Sotnikov, F. Frati, J. Okamoto, H. Y. Huang, A. Singh, D. J. Huang, K. Tomiyasu, C. H. Du, J. Kunes, and F. M. F. de Groot, Phys. Rev. B **98**, 035149 (2018).

[30] See the Supplementary Material at http://link.aps. org/supplemental/10.1103/PhysRevB.101.245162 for computational details and fitting analysis of the experimental data, which includes Refs. [44–49].

[31] N. B. Brookes, F. Yakhou-Harris, K. Kummer, A. Fondacaro, J. C. Cezar, D. Betto, E. Velez-Fort, A. Amorese, G. Ghiringhelli, L. Braicovich, R. Barrett, G. Berruyer, F. Cianciosi, L. Eybert, P. Marion, P. van der Linden, and L. Zhang, Nucl. Instrum. Methods Phys. Res., Sect. A **903**, 175 (2018).

[32] J. F. Afonso and J. Kuneš, Phys. Rev. B **95**, 115131 (2017).

[33] A. Georges, G. Kotliar, W. Krauth, and M. J. Rozenberg, Rev. Mod. Phys. **68**, 13 (1996).

[34] K. Byczuk and D. Vollhardt, Phys. Rev. B **77**, 235106 (2008).

[35] P. Anders, E. Gull, L. Pollet, M. Troyer, and P. Werner, Phys. Rev. Lett. **105**, 096402 (2010).

[36] P. Anders, E. Gull, L. Pollet, M. Troyer, and P. Werner, New J. Phys. **13**, 075013 (2011).

[37] W.-J. Hu and N.-H. Tong, Phys. Rev. B **80**, 245110 (2009).

[38] P. Werner, A. Comanac, L. de' Medici, M. Troyer, and A. J. Millis, Phys. Rev. Lett. **97**, 076405 (2006).

[39] B. S. Shastry, Phys. Rev. Lett. **107**, 056403 (2011).

[40] E. Perepelitsky and B. S. Shastry, Ann. Phys. (NY) **338**, 283 (2013).

[41] J. Fernández Afonso, A. Sotnikov, and J. Kuneš, J. Phys.: Condens. Matter **30**, 135603 (2018).

[42] V. Křápek, P. Novák, J. Kuneš, D. Novoselov, D. M. Korotin, and V. I. Anisimov, Phys. Rev. B **86**, 195104 (2012).

[43] K. Tomiyasu, T. Nomura, Y. Kobayashi, S. Ishihara, S. Ohira-Kawamura, and M. Kofu, arXiv:1808.05888.

[44] E. Gull, A. J. Millis, A. I. Lichtenstein, A. N. Rubtsov, M. Troyer, and P. Werner, Rev. Mod. Phys. **83**, 349 (2011).

[45] J. Kuneš, R. Arita, P. Wissgott, A. Toschi, H. Ikeda, and K. Held, Comput. Phys. Commun. **181**, 1888 (2010).

[46] A. Ikeda, T. Nomura, Y. H. Matsuda, A. Matsuo, K. Kindo, and K. Sato, Phys. Rev. B **93**, 220401 (2016).

[47] J. F. Afonso, A. Sotnikov, A. Hariki, and J. Kuneš, Phys. Rev. B **99**, 205118 (2019).

[48] A. A. Mostofi, J. R. Yates, G. Pizzi, Y.-S. Lee, I. S., D. Vanderbilt, and N. Marzari, Comput. Phys. Commun. **185**, 2309 (2014).

[49] M. Jarrell and J. Gubernatis, Phys. Rep. **269**, 133 (1996).